



Technical Note

Prediction of the resonance frequency of natural convection in an enclosure with time-periodic heating imposed on one sidewall

Ho Sang Kwak^{a,1}, Kunio Kuwahara^a, Jae Min Hyun^{b,*}

^aSpace Environment Laboratory, The Institute of Space and Astronautical Science, 3-1-1 Yoshinodai, Sagami-hara, Kanagawa 229, Japan

^bDepartment of Mechanical Engineering, Korea Advanced Institute of Science and Technology, 373-1 Kusong-dong, Yusong-gu, Taejeon 305-701, South Korea

Received 8 November 1996

Nomenclature

f frequency of the time-varying thermal boundary conditions, Fig. 1
 g gravitational acceleration
 H height of the cavity, Fig. 1
 k thermal conductivity
 L width of the cavity, Fig. 1
 n ratio of the horizontal wavenumber to the vertical wavenumber
 Pr Prandtl number, ν/χ
 q_m'' time-mean heat flux per unit area, Fig. 1 and Fig. 2
 Ra Rayleigh number based on the time-mean heat flux, $Ra = (\alpha g q_m'' H^4)/(k\nu\chi)$
 Ra_T Rayleigh number based on the time-mean temperature difference between the two sidewalls, $Ra_T = (\alpha g \Delta T_m H^3)/(\nu\chi)$
 T temperature
 t time
 v velocity
 x, y horizontal and vertical coordinates, Fig. 1.

Greek symbols

α volumetric expansion coefficient
 ΔT temperature difference between hot and cold sidewalls, Fig. 2

ε amplitude of the periodic heat flux or the wall temperature oscillation, Fig. 2
 χ thermal diffusivity
 ν kinematic viscosity
 θ non-dimensional temperature, $\theta = (T - T_c)k/(q_m'' H)$.

Subscripts

c cold sidewall
 h hot sidewall
 m time-mean value
 r resonance.

1. Introduction

In recent years, attention has been given to natural convection in an enclosure with time-periodic thermal boundary conditions [1–7]. Apart from the relevance of such boundary conditions to many practical applications [3, 5], these problems pose physically attractive issues mainly because of the possibility of resonance.

The pioneering work of Lage and Bejan [1] was the first to demonstrate the presence of resonance in natural convection. They considered a Boussinesq fluid in a square cavity with a constant-temperature cold sidewall and thermally-insulated horizontal endwalls. A periodic heat flux varying in a square wave fashion was imposed on the opposite sidewall (hereinafter referred to as model 1). Resonance was identified by the maximal amplification of fluctuations of the instantaneous Nusselt number, which was discernible at certain frequencies of forcing. Antohe and Lage [2, 3, 5] extended the concept of

* Corresponding author.

¹Current address: Supercomputer Center, Systems Engineering Research Institute, 1 Euen-dong, Yusong-gu, Taejeon 305-333, South Korea.

resonance for porous systems. For a related problem setup with the hot-wall temperature varying sinusoidally with time (referred to as model II), Kwak and Hyun [6] conducted comprehensive numerical simulations, which illustrated the existence of resonance. The flow configurations and the boundary conditions of models I and II are schematically depicted in Fig. 1.

More recently, Antohe and Lage [4] performed precision-controlled experiments for model I. It was found that for a high Rayleigh number, the time-mean heat transfer coefficient was augmented by periodic heating as compared with that obtained by steady heating with the same time-mean heat flux. In model II, Kwak *et al.* [7] revealed that the wall-temperature oscillation with a large amplitude causes an enhancement of the time-mean heat transfer rate. It is noted that the maximum gain of the time-mean heat transfer is obtained at the resonance frequencies [4, 7].

The previous results suggest that a proper utilization of resonance phenomenon may lead to an enhancement of heat transfer rate. An important element in this endeavor is an accurate prediction of the resonance

frequency, since the occurrence of resonance is sensitive to the forcing frequency. For model II, it was shown that the flow resonates with the internal gravity wave modes [6, 7]. Scaling analyses were also carried out to estimate the resonance frequency of model I [1–3, 5]. However, the predictions gave only the order of magnitude values. In the present study, based on a brief overview of the prior works [1–7], a prediction method to estimate the resonance frequency for model I is proposed.

2. Background review and strategy

Resonance describes a phenomenon in which the eigenmodes are amplified substantially if the system is periodically exposed to an external forcing with correct eigenfrequencies. For a system with fixed eigenfrequencies, the occurrence of resonance is largely independent of the amplitude of external forcing. The preceding works [3, 7] are supportive to this argument; in both models, the resonance frequency, f_r , is insensitive to the amplitude of the periodic thermal boundary conditions, ε .

The above considerations imply that f_r can be predicted by simply analyzing the solutions for the corresponding non-oscillating case with the same time-mean flux or wall temperature, i.e., $\varepsilon = 0$ (referred to as the basic state). This approach reduces considerable computational efforts required for searching for f_r by full numerical simulations covering a broad range of forcing frequency. This strategy was previously adopted in the earlier studies [1, 6]. The influence of ε on f_r , although minor, can also be assessed by scrutinizing the time-mean solution averaged over a cycle [7] or the upper and lower solutions with the boundary conditions $q'' = q''_m(1 \pm \varepsilon)$ [3].

In this study, the basic state solutions are used to estimate the resonance frequency. To this end, numerical solutions to the Navier–Stokes equations were obtained for the basic state solutions. A finite-volume procedure was employed, and the method in detail can be found in Kwak and Hyun [6]. (82×62) grid points were deployed for all computations.

Here, it is worth pointing out that the occurrence of resonance does not depend on the kind of external forcing. It is stressed that the difference between models I and II is only the type of thermal forcing. The fundamental physics of natural convection with a horizontal heat flux (model I) is qualitatively similar to those with a horizontal temperature difference (model II). There exists an analogy between these two problems [1–3]. The representative plots showing the flow patterns and temperature fields of the basic states of the two models are illustrated in Fig. 2, which exhibits similarities. This indicates that the resonance frequency of both models I and II may be predicted based on a similar physical ground.

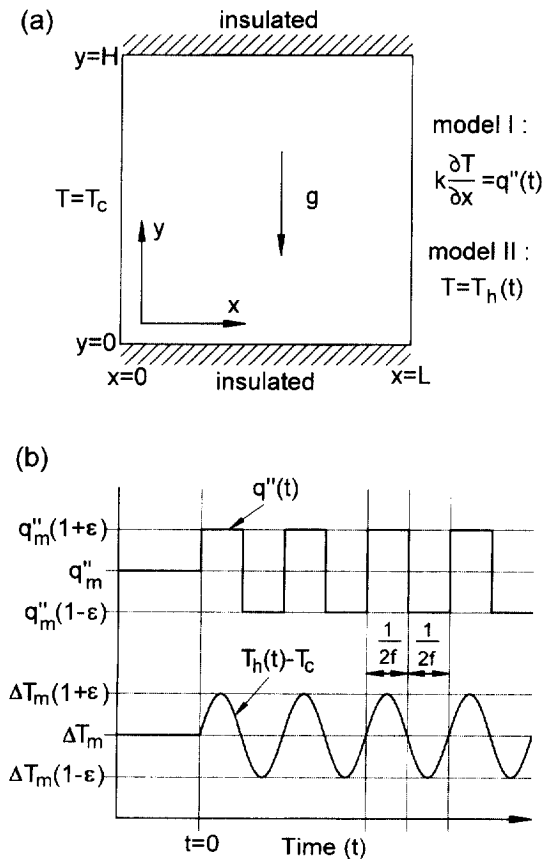


Fig. 1. (a) Schematic diagram of models I and II, and (b) the thermal boundary conditions imposed on the hot sidewall.

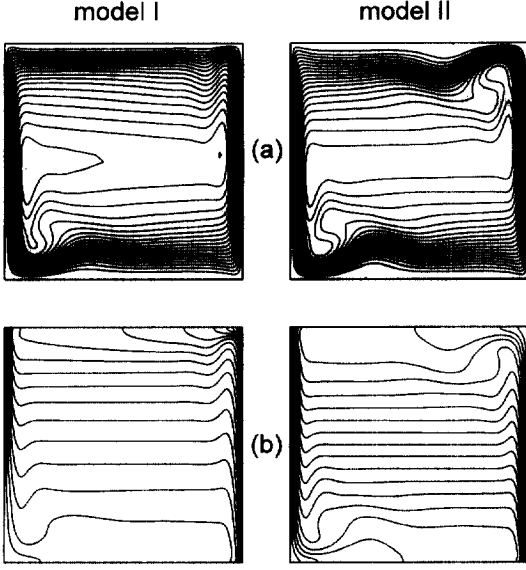


Fig. 2. (a) Flow patterns and (b) isotherms of the basic-state solutions of model I ($Ra = 10^8$, $Pr = 0.7$) and model II ($Ra = 10^7$, $Pr = 0.7$).

3. Prediction of the resonance frequency

Lage and Bejan [1] conducted a heuristic scale analysis, introducing the concept of the rotation of a fluid wheel. Resonance is to occur if the period of the cyclic heat flux coincides with the time duration over which the effects of cyclic heating rotate through the full cavity. The frequency of rotation of a fluid wheel was expressed as

$$f = \frac{v}{2(L+H)} \tag{1}$$

The baseline idea is physically reasonable, and the task is to select a proper scale for v .

Subsequently, Lage and Bejan [1] employed the longitudinal velocity in the vertical boundary layer as a scale for v . For model I, this velocity can be scaled as [1]:

$$v \sim \frac{\chi}{H} \left[\frac{Ra}{\xi(Pr)} \bar{\theta}_h \right]^{1.2} = \frac{x}{H} \left[\left(\frac{Ra}{\xi(Pr)} \right)^{4.5} \frac{L}{H} \right]^{1.2} \tag{2}$$

where $\bar{\theta}_h = (L/H)[Ra/\xi(Pr)]^{-1.5}$, $\xi(Pr) = 1$ for $Pr \geq 1$ and $\xi(Pr) = 1/Pr$ for $Pr < 1$.

Antohe and Lage [3] derived a scaling relationship to estimate v from the momentum equations and heat balance in the vertical boundary layers. For model I, this is

$$v^2 \left(1 + \frac{1}{1+L/H} \right) [1 + Pr\xi(Pr)] \sim \frac{\chi^2}{H^2} Ra Pr \xi(Pr) \bar{\theta}_h \tag{3}$$

The scalings in equations (2) and (3) are based on the velocities in the vertical boundary layers. The implication

is that the principal transport of the effects of periodic sidewall heating is accomplished by convective currents.

On the other hand, in the resonant cases of model II, the maximal fluctuations of flow and periodic tilting of isotherms were observed mainly in the interior, and the numerically-acquired resonance frequencies were in close agreement with the frequencies of internal gravity wave modes [6, 7]. These signify that the effects of periodic boundary conditions are delivered by the propagating modes of internal gravity waves. The afore-mentioned similarity between the two models, in particular, the stably-stratified temperature distribution in the interior, suggests that the resonance frequency of model I is also associated with the internal gravity wave modes.

The frequency of internal wave oscillation of an enclosed Boussinesq fluid can be deduced as [8]

$$f = \frac{1}{2\pi} \left[\alpha g \frac{\partial T}{\partial y} \frac{1}{(H/L) + n^2(L/H)} \right]^{1.2} \tag{4}$$

where n is the ratio of the horizontal wavenumber to the vertical wavenumber. For model I with $H/L = 1$, the frequency of the fundamental mode ($n = 1$) becomes

$$f = \frac{\chi}{H^2} \frac{\sqrt{2}}{4\pi} \left(Ra Pr \frac{\partial \theta}{\partial y} H \right)^{1.2} \tag{5}$$

In order to assess $\partial\theta/\partial y$, the method of Kwak et al. [6] is adopted. For all the sets of Ra and Pr examined by Lage and Bejan [1], the profiles of θ at the vertical plane ($x = L/2$) of the basic-state solutions are shown in Fig. 3. For $Pr = 0.01$, since no steady solutions were found,

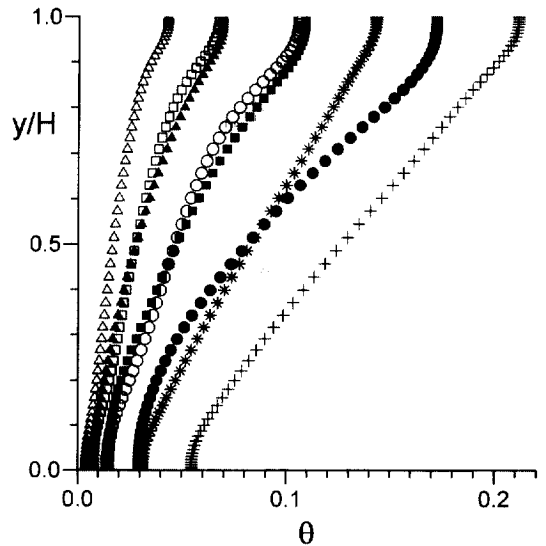


Fig. 3. Profiles of the temperature of the basic-state solutions ($x = 0$) at the vertical plane ($x = L/2$) for model I. \circ , $Ra = 10^7$, $Pr = 7.0$; \square , $Ra = 10^8$, $Pr = 7.0$; \triangle , $Ra = 10^9$, $Pr = 7.0$; \bullet , $Ra = 10^6$, $Pr = 0.7$; \blacksquare , $Ra = 10^7$, $Pr = 0.7$; \blacktriangle , $Ra = 10^8$, $Pr = 0.7$; $+$, $Ra = 10^6$, $Pr = 0.01$; $*$, $Ra = 10^7$, $Pr = 0.01$.

the time-averaged solutions at large times were plotted. The values of $\partial\theta/\partial y$ were evaluated by a linear fitting of temperature profiles near the geometric center, i.e., in the range $0.2 \leq y/H \leq 0.8$.

The predicted values of the resonance frequency, based on the above two different approaches, are compared in Table 1. The prediction by equation (5), in general, appears to give a better agreement with the numerical results of Lage and Bejan [1] than those by equations (1)–(3). For $Pr = 0.01$, considerable discrepancies are evident. A plausible explanation is that the pronounced inertia effects for low Pr produce different types of waves which would be more dominant than the internal gravity waves. However, the results for $Pr = 0.7$ and $Pr = 7.0$ give credence to the assertion that the resonance frequency is related primarily to the internal gravity wave oscillations. The slight differences between the estimated values of f_r and those of the detailed numerical computations [1] are attributable to the uncertainty in estimating the frequency of internal gravity waves, i.e., in determining $\partial\theta/\partial y$ by linear fitting of numerical data.

4. Conclusion

Based on the qualitative similarity of fundamental physics of natural convection in models I and II, a theoretical prediction was made of the resonance frequency in model I. The numerical solutions for the corresponding non-oscillating thermal boundary conditions ($\varepsilon = 0$) were analyzed. The estimated frequencies of internal gravity wave modes provided an improved prediction tool for the resonance frequencies in model I, in com-

parison to the previous attempts using scaling analyses [1, 3].

Acknowledgement

This work was supported in part by a grant from the Center of Excellence (COE) Program of the Ministry of Education, Science, Sports and Culture, Japan.

References

- [1] Lage JL, Bejan A. The resonance of natural convection in an enclosure heated periodically from the side. *Int J Heat Mass Transfer* 1993;36:2027–38.
- [2] Antohe BV, Lage JL. A dynamic thermal insulator: inducing resonance within a fluid saturated porous medium enclosure heated periodically from the side. *Int J Heat Mass Transfer* 1994;37:771–82.
- [3] Antohe BV, Lage JL. Amplitude effect on convection induced by time-periodic horizontal heating. *Int J Heat Mass Transfer* 1996;38:1121–33.
- [4] Antohe BV, Lage JL. Experimental investigation on pulsating horizontal heating of an enclosure filled with water. *ASME J Heat Transfer* 1996;118:889–96.
- [5] Antohe BV, Lage JL. The Prandtl number effect of the optimum heating frequency of an enclosure filled with fluid or with a saturated porous medium. *Int J Heat Mass Transfer* 1997;40:1313–23.
- [6] Kwak HS, Hyun JM. Natural convection in an enclosure having a vertical sidewall with time-varying temperature. *J Fluid Mech* 1996;329:65–88.
- [7] Kwak HS, Kuwahara K, Hyun JM. Resonance enhancement of natural convection heat transfer in a square enclosure. Revision submitted to *Int J Heat Mass Transfer*.
- [8] Paolucci S, Chenoweth DR. Transition to chaos in a differentially heated vertical cavity. *J Fluid Mech* 1989;215:379–410.

Table 1

Comparison of numerical and theoretical estimations of the resonance frequency. The values in () indicate the percentage errors relative to the numerical results of Lage and Bejan [1]

Pr	Ra	Resonance frequency, f_r , scaled by x/H^2			
		Numerical results of Lage and Bejan [1]	Theoretical prediction, equations (1) and (2)	Theoretical prediction, equations (1) and (3)	Theoretical prediction, equation (5)
7.0	10^7	251.0	157.7 (–37.2)	120.5 (–52.0)	265.0 (+5.6)
7.0	10^8	661.4	396.2 (–40.1)	302.6 (–54.3)	649.8 (–1.8)
7.0	10^9	1506.	995.3 (–33.9)	760.1 (–49.5)	1614. (+7.2)
0.7	10^6	41.83	54.45 (+30.1)	28.75 (–31.3)	40.31 (–3.6)
0.7	10^7	105.8	136.8 (+29.2)	72.23 (–31.8)	96.14 (–9.2)
0.7	10^8	209.2	343.5 (+64.2)	181.4 (–13.3)	235.2 (+12.4)
0.01	10^6	8.000	9.953 (+23.4)	1.817 (–77.3)	4.798 (–40.0)
0.01	10^7	14.86	25.00 (+68.2)	4.564 (–69.3)	12.65 (–14.9)